

# Toolchain Development for Automated Scene Reconstruction using Artificial Neural Network Object Detection and Photogrammetry for the Application in Driving Simulators

Maximilian Jarofka, Stephan Schweig, Niko Maas and Dieter Schramm  
*Chair of Mechatronics, University of Duisburg-Essen, Lotharstraße 1, 47057 Duisburg, Germany*

**Keywords:** Artificial Neural Network, COLMAP, Clustering, Driving Simulator, Metashape, Meshroom, Object Classification, Object Detection, Photogrammetry, Process Chain, Unity, VisualSFM.

**Abstract:** This paper presents an automated process chain for the reconstruction of characteristic 3D objects, which can be used in a simulation environment. The process chain can distinguish between recurring objects such as trees and cars and specific objects like buildings. To acquire this, it detects and classifies objects in images from a previously recorded video. In contrast to the specific objects, which are reconstructed during the workflow of the process chain, the recurrent objects are loaded from already existing models and are placed multiple times into the simulation environment. In terms of quality a visual comparison between the two integrated programs for the reconstruction (Metashape and Meshroom) is carried out. Furthermore the accuracy of the positioning of standard objects in the Unity game engine is examined.

## 1 INTRODUCTION

Today driving simulators are used in a wide variety of areas. In the industry they are used, for example, to simulate ships or to simulate the driving behaviour of road vehicles. Furthermore, they serve as training devices for new drivers in uncommon or dangerous situations. One big advantage of using simulators is the reproducibility of different test scenarios, as well as the secure simulation of risky situations. This paper describes the development of an automated process chain for object reconstruction on the example of an automotive driving simulator.

Simulators benefit from the rapid development of the computing power of microchips. Therefore, the demands on the developed scenarios, especially with regard to graphical details, are growing to the same extend. To make the test drive within a driving simulator as realistic as possible, a detailed graphical simulation environment must be provided.

Those scenarios consist of different types of objects. On the one hand, there are recurring objects such as trees, cars or street lights. By loading them from an object database they can be placed in the environment. To ensure a variation in the build scenario, their individual properties such as colour or shading can be modified. On the other hand, there are specific

objects, which cannot be replaced by objects from a database or loaded multiple times into the simulation environment due to their uniqueness. Therefore these objects have to be modelled individually. If a simulation should be based on a real environment (e.g. streets of an existing city), concise objects, such as buildings, have to be modelled. This process does not only take much time but also requires considerable know-how in 3D modelling.

This paper presents an automated procedure for the reconstruction of 3D objects and their integration into a scenario. The automation is intended to make the design of scenarios for driving simulators more efficient and therefore less time consuming. The automated process chain is based on recorded data from a ZED stereoscopic camera, manufactured by Stereolabs (Stereolabs Inc., 2020). From this dataset, the process chain will reconstruct specific objects and imports them into a Unity scene along with standard objects like cars and trees, loaded from previously existing models.

In the first step objects and their three-dimensional positions have to be determined. Afterwards, by applying photogrammetric methods, the objects are reconstructed. Purpose of the developed process chain is the generation of a scenario which can directly be used as a simulation environment.

## 2 STATE OF THE ART

In this section, the theoretical concepts of this paper are explained. Objects within recorded images are detected automatically and subsequently reconstructed to 3D models. An object classifier based on an artificial neural network is used for the detection of these objects.

Therefore the basics of the used object classifier are explained in the first subsection. Furthermore the basic principles of photogrammetric methods are stated. Through the use of these methods, the recognized objects are transformed into 3D models.

### 2.1 Object Detection and Classification

There are big improvements in the field of object recognition and computer vision in general. One reason for these improvements is the increase in computing power and thus the associated possibility to use deeper artificial neural networks, (He et al., 2016)

For the detection and classification of objects the artificial neural network with the name "You Only Look Once (YOLO)" is used in this work. This network was originally developed in the year 2015 and is now published in the third version, (Redmon et al., 2015; Redmon and Farhadi, 2016; Redmon and Farhadi, 2018). The actual version of YOLO consists of a large number of hidden layers. Figure 1 shows the detailed structure of the network.

This specific system has a number of features that distinguish it from other object classifiers. Different bounding boxes are predicted in a single evaluation of the source image. A probability value is assigned to each of them. This value represents the combined probability of the object being correctly mapped and the correct assignment of an object class.

In contrast to this procedure other systems run a classifier over the input image at predefined intervals to perform object detection at each of these points. As a result, the detection process takes comparatively long. Also other systems often consist of a sequence of different processes which form a process chain. The resulting interdependencies between different process parts make it very difficult to improve the overall performance in one step. The YOLO object detection system however, consisting of a single network, makes it easy to apply known strategies from the field of artificial neural networks for improving performance, (Redmon and Farhadi, 2018).

The results of the classification process with YOLO are bounding boxes. Each box contains the location in image coordinates (X,Y) and the width and height of the box in pixels. In addition, a bound-

	Type	Filters	Size	Output
	Convolutional	32	3 × 3	256 × 256
	Convolutional	64	3 × 3 / 2	128 × 128
1×	Convolutional	32	1 × 1	
	Convolutional	64	3 × 3	
	Residual			128 × 128
	Convolutional	128	3 × 3 / 2	64 × 64
2×	Convolutional	64	1 × 1	
	Convolutional	128	3 × 3	
	Residual			64 × 64
	Convolutional	256	3 × 3 / 2	32 × 32
8×	Convolutional	128	1 × 1	
	Convolutional	256	3 × 3	
	Residual			32 × 32
	Convolutional	512	3 × 3 / 2	16 × 16
8×	Convolutional	256	1 × 1	
	Convolutional	512	3 × 3	
	Residual			16 × 16
	Convolutional	1024	3 × 3 / 2	8 × 8
4×	Convolutional	512	1 × 1	
	Convolutional	1024	3 × 3	
	Residual			8 × 8
	Avgpool		Global	
	Connected		1000	
	Softmax			

Figure 1: Layers of the artificial neural network YOLO version 3 (Redmon and Farhadi, 2018).

ing box also contains an object class and a probability information about the correct mapping of the object. This probability considers (as already mentioned above) the correct position and class of the object. Figure 2 shows possible object detections and their visualization in the original image.

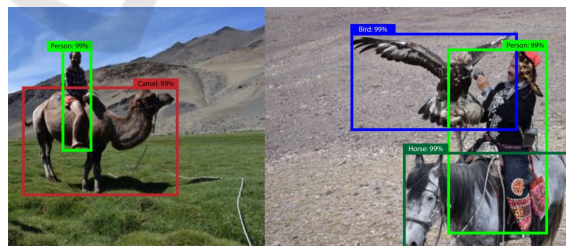


Figure 2: Detected objects in original picture (Redmon and Farhadi, 2018).

Which objects can be recognized by the system depends on the training data used. Like the human brain, the network must first "learn" the detection of specific objects. In this paper the artificial neural network YOLOv3, pre-trained on the open-image dataset is used. With this version it is possible to recognize and classify 601 different objects (Kuznetsova et al., 2018).

## 2.2 Photogrammetry

Photogrammetry originally describes the measurement of various properties of an object from images. Today the term "photogrammetry" is mostly used to describe the determination of three dimensional coordinates from different images of an object without any physical contact. Thus it is possible to reconstruct complete 3D models of these objects. Depending on the camera used (standard digital camera or special measuring camera) very high accuracies of these models can be achieved, (Donath, 2009).

Since the first developments in the field of photogrammetry, those methods have established themselves as an important and widely used tool. A special approach within photogrammetry is the so called Structure-from-Motion method (SfM), (Westoby et al., 2012).

In contrast to other photogrammetric methods, such as stereoscopic photogrammetry, a process chain containing SfM offers several advantages. By using SfM methods, it is possible to reconstruct a 3D object without prior knowledge of the position and orientation of the images taken. This means, that objects can be captured with standard cameras (without any further sensory setup such as GPS or gyroscope) and then be reconstructed into a 3D model, (Westoby et al., 2012; Shashi and Jain, 2007).

The term "Structure-from-Motion" here denotes that 3D structures are reconstructed from the movement of the camera and the resulting different angles of view in each image, (Szeliski, 2010).

The entire process, from reading the individual images to the finished 3D model, often is denoted as Structure from Motion. More precisely, however, SfM is only an intermediate step in the entire process chain. The camera position, as well as the position of the feature coordinates in a uniform coordinate system, are determined from a priori detected geometrical features. Subsequently, a point cloud can be created to link these to a 3D model and texturing can be used to create a final 3D model.

The flowchart shown in Figure 3 describes a possible photogrammetric process chain using SfM algorithms as used in the AliceVision-Framework (AliceVision, 2020).

## 3 AUTOMATED PROCESS CHAIN

Within this section, the basic procedure of an automated scenario reconstruction is presented. A process chain is developed by which individual objects can be detected and reconstructed. Subsequently, these ob-

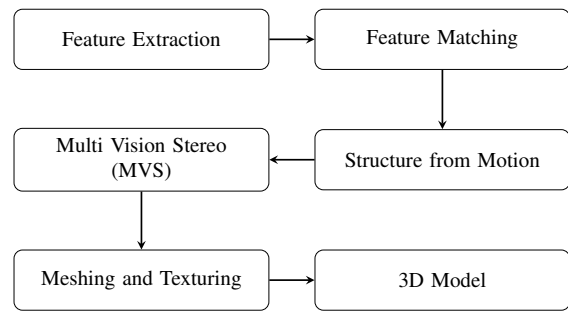


Figure 3: Flowchart of a possible SfM process chain (AliceVision, 2020).

jects are assembled to a scenario in the Unity game engine.

The process chain consists of a higher-level program that calls and controls various subprograms. The objective is to make the sequential flow of all programs as independent from user interaction as possible. For this purpose, all important parameters are collected within a configuration file. This allows the user to specify all parameters in advance and then run the process chain unattended.

In addition to the high degree of automation, the process chain should also have the highest possible degree of modularity. It should be possible to start individual steps without the preceding ones. This modular structure is very useful for adapting the parameters in test runs. If some steps of the process chain have already been completed successfully, only the following module can be started with adapted parameters. Thus, already completed steps do not have to be repeated and the processing time is reduced.

Furthermore, the modular structure enables an interruption of the process chain at any point and the continuation at another time. However, since the sequence cannot be changed due to the dependencies of the individual steps, the modules must be processed one after the other and cannot be executed in parallel (except the object detection/clustering and the data extraction as seen in Figure 4). To activate each module individually, the configuration file contains the parameter *run = true/false* for each module. Only the modules with the parameter *run = true* are executed within the process chain.

Figure 4 shows the process chain as a flow chart. The different labels within this diagram represent different types of subroutines. The hatched fields represent self developed scripts. They are used to control an already existing software - such as Unity, Blender or Metashape (Agisoft LLC, 2020; AliceVision, 2020). The script enables the transfer of required parameters to the respective program. A specific programming interface of the program is then

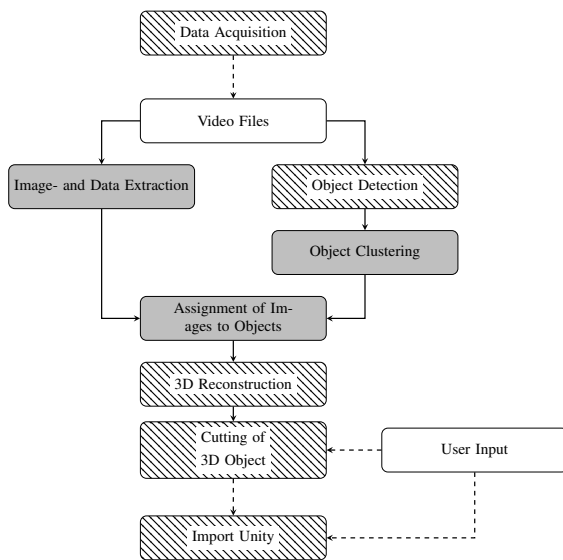


Figure 4: Flowchart of the developed process chain.

used to run the intended sub tasks. Fields highlighted in grey represent own programs, which were developed especially for the integration in the process chain.

In addition to the programs listed here, there is another program that controls the entire process chain. This program runs the individual sub-programs/subscripts with corresponding parameters loaded from the configuration file.

Splitting the task in different sub tasks ensures the above-mentioned flexibility of the process chain. Another important factor in the development of the process chain is the independence from direct user input. As seen in Figure 4, only the cutting of 3D model and the start of the import process of the objects into the Unity game engine require direct user interaction.

In the following subsection only the most important parts of the process chain are explained in more detail. Thus the object detection, object clustering and 3D reconstruction are discussed further on.

### 3.1 Object Detection

To start the object detection, the corresponding Python script in the installation folder of YOLO is started by the main program. This is a version that has been specially modified for the purposes of the automated process chain. The original script for the integration of the used stereoscopic camera in the YOLO-workflow can be downloaded from GitHub, (AlexeyAB, 2018).

For each detected object the artificial neural network provides specific values. In addition to the classification (e.g. *tree*), size of the bounding box (in

pixels) and position (in pixels) of the object, a value for the accuracy of the detection is available. This is a percentage value that indicates the certainty of a correct classification. By selecting an appropriate *Threshold* parameter in the configuration file, the objects can be filtered according to these values. Only detections of objects with a certainty above the value of the *Threshold* parameter are considered as correct and will be saved. Initial tests have shown that a *Threshold* of roughly 0.3 seems to be well suited for the detection of buildings on the roadside.

To store the object information, a simple text document is created for each processed video file. For each recognized object within each image one line with its information is stored. An example for such entries is shown in Table 1. In addition to the number of the image in which the object was detected, the information about its mean position within the image ( $X$ ,  $Y$ , height, width) also its position in three-dimensional space ( $Pos_X$ ,  $Pos_Y$ ,  $Pos_Z$  in meters) is stored. To calculate this 3D position of the object in world coordinates, the point cloud of the respective stereo image pair is used. The point cloud can be read out directly via a software function provided with the ZED camera.

The point cloud generated by the camera only contains a certain distance range. All pixels whose calculated distance to the camera is too small or too large, are not displayed in this point cloud. If a pixel is outside the point cloud, the value -1 is returned for its position. In table 1, this is the case for the object in the third line. The detected plant is too far away from the camera and its position, as well as other calculated parameters, are set to the error value of -1. In the following, such an object is considered as invalid and can be excluded by the parameter *includeInvalid=false* in the configuration file.

Furthermore the occlusion between two objects is calculated. A percentage value for the overlapping areas of both objects is determined if an object is occluded by another one in front of it. In further updates of the process chain an automated selection of the objects which should be reconstructed could be implemented based on this value.

### 3.2 Object Clustering

In the previous step, objects within individual images were detected and their position in the world coordinate system is calculated. Since the same object occurs in different images, the object positions must be clustered. As long as the positions of detected objects are close enough to one another, they are assigned to one object cluster. If a considered point lies within a

Table 1: Object information saved by the YOLO script.

Nb.	Class	Accuracy	X	Y	Width	Height	Pos <sub>X</sub>	Pos <sub>Y</sub>	Pos <sub>Z</sub>	Distance	Occlusion
1485	Building	38.0	861	131	411	533	-60.256	7.155	-28.700	11.285	0.307
1485	Building	36.0	0	137	587	510	-71.969	10.201	-41.555	20.350	0.107
1485	Plant	27.0	560	238	196	253	-1	-1	-1	-1	-1
1485	Car	26.0	490	522	186	110	-67.236	5.014	-29.367	7.535	0.0
1485	Plant	20.0	924	469	344	243	-63.875	4.727	-26.113	6.643	0.0

certain radius to any point in a cluster, it is also assigned to it. Cloudlike object boundaries are created, (compare Figure 5).

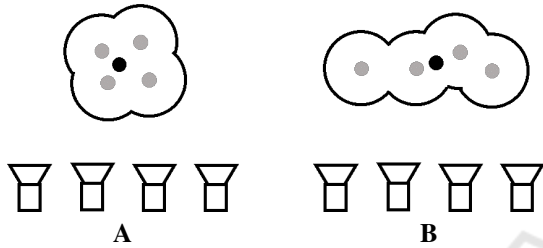


Figure 5: Visualization of the clustering process.

In addition to characteristic delimitations, two different cases of clustering can be seen in Figure 5. Scenario **A** is a single smaller object that was recorded from all camera perspectives. Due to inaccuracies in the image recording or object recognition, deviations of the object positions in the world coordinate system (gray dots) occur. However, each of these positions is within the threshold (radius) to a different point. Therefore, all points are combined into a common cluster (and thus into one object) with an averaged centre position (black point).

Scenario **B** is a continuous object that is too big to be captured in one image. YOLO detects the object approximately over the entire width of the respective image. This results in points shifted parallel to the movement of the camera. Just like scenario **A**, however, these are within the selected threshold and are thus assigned to one and the same object. This procedure for clustering objects makes it possible to cluster even larger objects correctly, which span over several images.

In addition to the threshold value for the proximity of all points to one another, a further threshold value for the number of points is introduced. Individual clusters are only considered as correct if the number of points in them exceeds the threshold value. This means that individual faulty detections are not considered as a separate cluster with a very small number of individual points.

The program for creating the object clusters first reads the files with the information about all detected objects (compare section 3.1). A label for the clus-

tering can now be specified via the configuration file. If an object does not have the appropriate label, it is discarded and not assigned to a cluster. If all objects have been distributed to the clusters or have been discarded, the clusters with too few individual objects are also discarded. The mean value of the position is now calculated for all remaining clusters. The resulting averaged objects are then saved in another text file. Simultaneously to the positions and other information, all image numbers in which the respective object occurs are saved. Using these numbers, the extracted images can be split up and further be processed to reconstructed objects using photogrammetry.

### 3.3 3D Reconstruction

In order to determine a suitable reconstruction program for the use within this process chain, some preliminary tests were carried out during its development. At first, different software solutions for the reconstruction of 3D models were tested. The used camera already comes with software for 3D reconstruction. It is integrated in the software development package and already has a graphical user interface. It uses the point clouds generated by the stereo camera for the reconstruction of objects. However, it was not able to provide usable models in initial tests and was therefore not considered further for the use within the process chain. In addition, the programs VisualSFM (Wu, 2013; Wu et al., 2011) and COLMAP (Schonberger and Frahm, 2016) were tested in advance. They were also unable to deliver satisfying results in initial tests and were therefore also not considered for further use in the process chain.

All the above mentioned programs delivered 3D models with many holes in the reconstructed surfaces as well as faulty textures. The minimum requirements for the generated models are a continuous surface and correct texturing. Furthermore, the texture of the objects should not overlap with textures from objects which are in front of them.

The first program to achieve acceptable results under these aspects was Metashape (Agisoft LLC, 2018). For this reason, the process chain was initially developed using this program. However, since it is a software that requires a licence, the program Mesh-

room was also tested and integrated into the process chain. It is a free open-source software which uses the AliceVision-Framework (AliceVision, 2020). Meshroom also allows the reconstruction of acceptable 3D models.

## 4 EXPERIMENTAL RESULTS

After the explanation of the developed automated process chain in the previous chapter, this chapter deals with some selected experiments carried out with it.

As described in section 3.1 the two already integrated programs in the process chain are Metashape and Meshroom. In the first section of this chapter they are compared in concerning the resulting 3D models.

Besides the reconstruction of objects by photogrammetric methods, the developed process chain also allows multiple imports of existing standard objects into the scene.

Therefore the second section of this chapter deals with the accuracy of this import procedure.

### 4.1 Comparison between the Two Integrated Reconstruction Programs

A uniform test procedure was defined, so that the two programs can be compared with each other. In the first part of the test runs, the standard process chain was applied several times to the same scenario. The number of images used and their resolution were varied. Through this procedure the results can be evaluated in terms of quality.

In order to guarantee constant conditions for the reconstruction programs, the process chain was only carried out up to the partial step of assigning the images to a specific object. Afterwards the test runs were carried out for both programs with a varying number of images. For this purpose the parameter *SkipCount* in the section *[Imagecopy]* of the configuration file was varied. This means that only every  $n^{th}$  frame from the video file is used for the reconstruction.

A street with three buildings on the side was chosen as the test scenario. To minimize the time required for all test runs, only the building in the middle was reconstructed. For better illustration it was roughly cut into shape in a manual step. The recorded screenshots of the respective building can be visually compared with each other with regard to quality.

The scenario above was recorded in two different resolutions. 720p as a medium resolution and 2.2K as maximum resolution delivered by the camera. Table 2

shows the resulting matrix for all test runs carried out with each reconstruction program.

Table 2: Example for one test matrix.

SkipCount	2	5	10	20
Nb of images (720p)	566	228	114	58
Nb of image (2.2K)	162	66	34	18

Figures 6 and 7 show exemplary reconstructed 3D models for the largest number of images at the medium resolution of 720p.



Figure 6: Resulting 3D model from Metashape (resolution 720p).

A direct comparison of the two models reveals differences in quality. The program Metashape (Figure 6) delivers better quality results than Meshroom (Figure 7). The boundaries of the object are less uneven. Also the actual flat surfaces of the building appear much smoother in the reconstruction of Metashape. Besides the unevenness of the boundaries and surfaces, the texture of the model in Figure 6 also appears sharper and less blurred.

In the second part of the tests, all runs were performed with the data recorded in the maximum resolution of 2.2K. The results of the two reconstruction programs will be compared with each other again for the largest number of used images.

Figures 8 and 9 show the resulting 3D models with the highest number of images used.

Overall, this comparison reveals similar differences. Again, the building facades from Metashape were reconstructed less uneven. The boundaries and edges of the building are also much clearer. This is

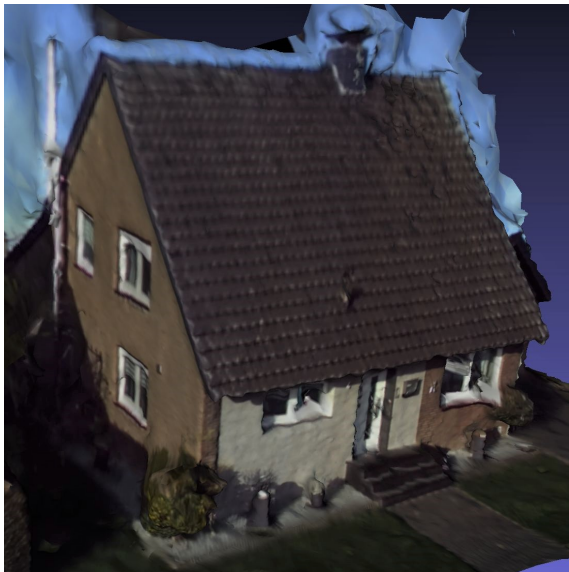


Figure 7: Resulting 3D model from Meshroom (resolution 720p).

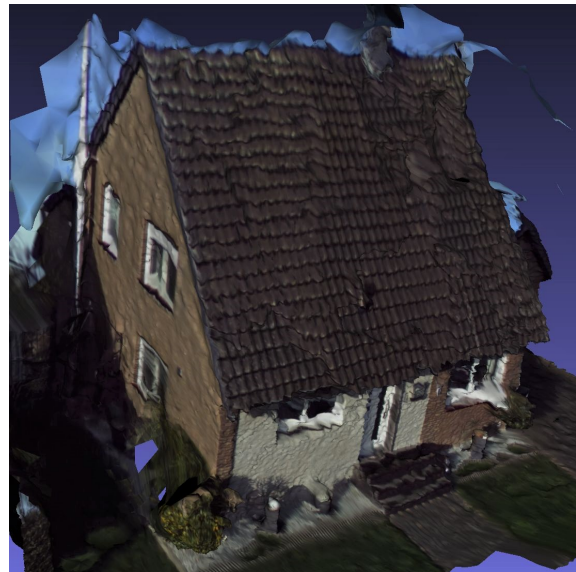


Figure 9: Resulting 3D model from Meshroom (resolution 2.2K).



Figure 8: Resulting 3D model from Metashape (resolution 2.2K).

particularly noticeable in the transition between the building and the sky. If all parts of the reconstructed sky were removed, Metashape would have a relatively straight edge. The reconstruction with Meshroom on the other hand has a much more uneven and jagged roof edge.

The tests with less images used for the reconstruction showed similar results. In general Metashape delivered better quality in all reconstructions. With a very low number of images the overall quality was re-

duced. Less than 66 images led to many holes and artefacts in the resulting 3D models.

In general it can be stated, that contrary to expectations, the quality is not improved by using the higher camera resolution. By using the maximum resolution, the quality of the reconstructed models is worse. Especially the frontal facade of the building shows considerably more unevenness. Also the floor is more uneven when using the higher resolution and is showing single gaps that were not reconstructed correctly.

In all reconstructed models, artefacts arise between the object and its surroundings. With regard to the reconstructed building, this is particularly noticeable in the transition from the building to the sky. In the immediate vicinity of the building, parts of the sky are also reconstructed. In the course of quality assessment these artefacts will not be considered. Since the creation of these artefacts cannot be prevented in both programs, they must be removed in the process of manual cutting anyway. Thus they do not represent an explicit characteristic of quality in a direct comparison.

## 4.2 Positioning of Standard Objects into the Game Engine Unity

With the developed automated process chain it is also possible to import recurring objects. As already mentioned above, objects can be recognized with YOLO and then be replaced by prefabricated 3D models at the corresponding positions within the scene. Regarding poly count and effective modelling, this allows the

models to be optimized in advance.

In the following section, the detection of such standard objects and their import are discussed. The tests were performed for the detection of cars at the roadside of the recorded scene. However, it is theoretically possible to use any of the object classes detectable by YOLO, see (Kuznetsova et al., 2018).



Figure 10: Imported standard objects at the detected positions of cars along a street.

Example objects are imported into the reconstructed scenario to visualize the detected positions. They consist of a long cylinder and a sphere. In Figure 10 it is clearly visible that the detected positions do not match the actual positions of the objects in the scene. They are shifted by a constant factor (here 4 m) along the x-axis. If the shift is corrected the calculated positions match the positions of the reconstructed model. A possible reason for the necessary correction is the general positioning of the 3D model. On the one hand, the reconstructed model has a specific coordinate system given by the reconstruction program. On the other hand, the objects are referenced to the coordinate system of the camera. Therefore, it is necessary to convert between the two coordinate systems.

In the current version of the process chain this is done by taking the positional information of only one image. If this is inaccurately aligned by the reconstruction program or the information itself is inaccurate, the whole model can easily be shifted.

In a second test scenario the positions of cars are examined again. This time using a straight building facade. Figure 11 shows the resulting point cloud for the selected scenario. The positions of the cars, which have to be detected, were marked manually by a red

circle and the automatically calculated positions were marked by loading the sample objects. When comparing the respective positions, differences are noticeable depending on the camera path covered. At the beginning of the recording (right part of Figure 11), the automatically determined positions almost match the manually marked positions. With increasing distance covered by the camera, however, the positions deviate more and more from each other. The automatically calculated position of the last car deviates about 10 meters from the manually marked position.

The actual course of the recorded facade is completely straight and without curves. In the point cloud shown, however, a bend to the right is clearly visible.

## 5 CONCLUSION

In the course of this paper a process chain for the automated reconstruction of 3D models and integration into a simulation environment is presented. The process chain uses data recorded from a stereoscopic camera. By using the YOLO artificial neural network, the process chain recognizes individual objects within the video frames and clusters them. Specific objects - such as buildings - getting converted into a 3D model by a 3D reconstruction program using photogrammetric methods. In addition to the object itself, its three-dimensional position is calculated and saved. For this purpose, the positional tracking of the stereoscopic camera is used. Based on this position, the object can be imported into a Unity scene. With the exception of cutting the raw mesh and starting the import process, the process chain is fully automated and does not require any user input.

To allow a certain modularity besides the automation, independent programs and scripts were developed. They were combined into a process chain by developing a supervising control program. The used parameters of all programs were combined in two configuration files for easy handling. The flow of the process chain already can be changed by adjusting various parameters. This also makes it possible to reconstruct scenarios coherently. Connected building facades can thus be reconstructed by adjusting only one parameter in a coherent model. It is also possible to reconstruct a scene from different camera angles. With the current design of the process chain, it is already possible to use a large number of cameras.

For the actual reconstruction of the 3D models, existing programs within the process chain are used. Two different reconstruction programs have already been integrated into the workflow. On one hand, the proprietary program Metashape from Agisoft can be





Figure 11: Imported standard objects at the detected positions of cars along a facade.

used. A corresponding license with access to the Python API must be available to use it. On the other hand, the free open-source program Meshroom can be used for reconstruction.

The differences between the two used programs were examined in detail. For all examples used in this work, the proprietary program Metashape generally gave better results.

By calculating the occlusion of individual objects, it is already possible to roughly divide the various objects within a scene according to the ability of being reconstructed. It can already be estimated if an object is suitable for reconstruction or whether it is too much hidden by other objects in front of it.

Furthermore, with the scripts created in this work, it is possible to cut the resulting 3D models and import them into the game engine Unity via a created graphical user interface. Not only newly reconstructed models can be imported during the process chain. It is also possible to import detected, recurring objects in the form of standard objects.

It was shown that the calculation of the object positions within certain scenarios already matches the recorded data with sufficient accuracy. Standard objects can thus be included in newly reconstructed scenarios but they require some manual corrections by the user to compensate the shift. For the placement of the reconstructed 3D objects, however, only a single position specification is used so far. Depending on the accuracy of the image arrangement within the reconstruction program, this can lead to a general inaccuracy in positioning, especially in the case of longer, connected objects.

During the recording of connected building facades, general position deviations were also detected. The position calculated by the camera deviates more and more from reality during the recording of house facades. Due to the rearrangement of the images during the reconstruction of the 3D objects, the positions subsequently deviate more with increasing cam-

era movement. The objects can therefore only be approximately positioned.

## 6 OUTLOOK

Autonomous inland shipping is currently being researched in the ongoing project "Autonomes Binnenschiff – Simulation und Demonstration von automatisiertem Fahren in der Binnenschifffahrt". Sensors from a real prototype ship are simulated to validate and improve the control algorithms. Afterwards these algorithms are tested in the simulation and on the ship. Especially for the cameras, the simulation environment has to be as realistic as possible with photo-realistic textures and objects. In this research project, the presented process chain will be adapted to the changed environment and used to simplify the generation of it.

Further development of the entire process chain will be carried out besides these specific adaptations. By implementing the automatic evaluation of the suitability for reconstruction and the resulting models themselves, the degree of automation will be further increased. Next to this evaluation, using the already calculated occlusion value, all used images will be evaluated in terms of quality. Bad images, such as blurry ones, will be discarded in further updates of the process chain.

Through the use of additional sensors, such as differential GPS, gyroscope and accelerometer, the positioning of the reconstructed objects will be further improved. Furthermore multiple images and their corresponding positions in real world coordinates will be regarded for the reconstruction process.

## ACKNOWLEDGEMENTS

The ongoing research in the project "Autonomes Binnenschiff – Simulation und Demonstration von automatisiertem Fahren in der Binnenschiffahrt", in which the presented process chain will be used and improved, is funded by the European Regional Development Fund (ERDF).

## REFERENCES

- Agisoft LLC (2018). *Agisoft Metashape User Manual, Professional Edition*, 1.5 edition.
- Agisoft LLC (2020). Agisoft metashape. <https://www.agisoft.com/>; Last visited 06.03.2020.
- AlexeyAB (2018). Github zed-yolo. <https://github.com/stereolabs/zed-yolo>; Last visited 31.01.2020.
- AliceVision (2020). Alicevision, meshroom. <https://alicevision.org>; Last visited 06.03.2020.
- Donath, D. (2009). *Photogrammetrie*. Vieweg+Teubner, Wiesbaden.
- He, K., Zhang, X., Ren, S., and Sun, J. (2016). Deep residual learning for image recognition. In *Proceedings of the IEEE conference on computer vision and pattern recognition*, pages 770–778.
- Kuznetsova, A., Rom, H., Alldrin, N., Uijlings, J. R. R., Krasin, I., Pont-Tuset, J., Kamali, S., Popov, S., Mallocci, M., Duerig, T., and Ferrari, V. (2018). The open images dataset V4: unified image classification, object detection, and visual relationship detection at scale. *CoRR*, abs/1811.00982.
- Redmon, J., Divvala, S. K., Girshick, R. B., and Farhadi, A. (2015). You only look once: Unified, real-time object detection. *CoRR*, abs/1506.02640.
- Redmon, J. and Farhadi, A. (2016). YOLO9000: better, faster, stronger. *CoRR*, abs/1612.08242.
- Redmon, J. and Farhadi, A. (2018). Yolov3: An incremental improvement. *arXiv preprint arXiv:1804.02767*.
- Schonberger, J. L. and Frahm, J.-M. (2016). Structure-from-motion revisited. In *Proceedings of the IEEE Conference on Computer Vision and Pattern Recognition*, pages 4104–4113.
- Shashi, M. and Jain, K. (2007). Use of amateur cameras in architectural photogrammetry. In *Map World Forum, Hyderabad, India*.
- Stereolabs Inc. (2020). Stereolabs zed 2k stereo camera. <https://www.stereolabs.com/>; Last visited 07.02.2020.
- Szeliski, R. (2010). *Computer Vision: Algorithms and Applications*. Springer-Verlag, Berlin, Heidelberg, 1st edition.
- Westoby, M. J., Brasington, J., Glasser, N. F., Hambrey, M. J., and Reynolds, J. (2012). Structure-from-motion photogrammetry: A low-cost, effective tool for geoscience applications. *Geomorphology*, 179:300–314.
- Wu, C. (2013). Towards linear-time incremental structure from motion. In *2013 International Conference on 3D Vision-3DV 2013*, pages 127–134. IEEE.
- Wu, C., Agarwal, S., Curless, B., and Seitz, S. M. (2011). Multicore bundle adjustment. In *CVPR 2011*, pages 3057–3064. IEEE.